



HAL
open science

Association of plasma YKL-40 with brain amyloid- β levels, memory performance, and sex in subjective memory complainers

Andrea Vergallo, Simone Lista, Pablo Lemercier, Patrizia A. Chiesa, Henrik Zetterberg, Kaj Blennow, Marie-Claude Potier, Marie-Odile Habert, Filippo Baldacci, Enrica Cavedo, et al.

► To cite this version:

Andrea Vergallo, Simone Lista, Pablo Lemercier, Patrizia A. Chiesa, Henrik Zetterberg, et al.. Association of plasma YKL-40 with brain amyloid- β levels, memory performance, and sex in subjective memory complainers. *Neurobiology of Aging*, 2020, 96, pp.22-32. 10.1016/j.neurobiolaging.2020.07.009 . hal-03491473

HAL Id: hal-03491473

<https://hal.science/hal-03491473>

Submitted on 21 Feb 2023

HAL is a multi-disciplinary open access archive for the deposit and dissemination of scientific research documents, whether they are published or not. The documents may come from teaching and research institutions in France or abroad, or from public or private research centers.

L'archive ouverte pluridisciplinaire **HAL**, est destinée au dépôt et à la diffusion de documents scientifiques de niveau recherche, publiés ou non, émanant des établissements d'enseignement et de recherche français ou étrangers, des laboratoires publics ou privés.



HAL
open science

Association of plasma YKL-40 with brain amyloid- β levels, memory performance, and sex in subjective memory complainers

Andrea Vergallo, Simone Lista, Pablo Lemercier, Patrizia Chiesa, Henrik Zetterberg, Kaj Blennow, Marie-Claude Potier, Marie-Odile Habert, Filippo Baldacci, Enrica Cavedo, et al.

► To cite this version:

Andrea Vergallo, Simone Lista, Pablo Lemercier, Patrizia Chiesa, Henrik Zetterberg, et al.. Association of plasma YKL-40 with brain amyloid- β levels, memory performance, and sex in subjective memory complainers. *Neurobiology of Aging*, 2020, 96, pp.22 - 32. 10.1016/j.neurobiolaging.2020.07.009 . hal-03769553

HAL Id: hal-03769553

<https://hal.science/hal-03769553>

Submitted on 14 Sep 2022

HAL is a multi-disciplinary open access archive for the deposit and dissemination of scientific research documents, whether they are published or not. The documents may come from teaching and research institutions in France or abroad, or from public or private research centers.

L'archive ouverte pluridisciplinaire **HAL**, est destinée au dépôt et à la diffusion de documents scientifiques de niveau recherche, publiés ou non, émanant des établissements d'enseignement et de recherche français ou étrangers, des laboratoires publics ou privés.



Distributed under a Creative Commons Attribution-NonCommercial 4.0 International License

Association of plasma YKL-40 with brain amyloid- β levels, memory performance and sex in subjective memory complainers

Andrea Vergallo^{1,2,3,*} §, Simone Lista^{1,2,3} §, Pablo Lemerrier^{1,2,3},
Patrizia A. Chiesa^{1,2,3}, Henrik Zetterberg^{4,5,6,7}, Kaj Blennow^{4,5}, Marie-Claude Potier⁸,
Marie-Odile Habert^{9,10,11}, Filippo Baldacci^{1,2,3,12}, Enrica Cavedo^{1,2,3},
Filippo Caraci^{13,14}, Bruno Dubois^{1,2,3}, and Harald Hampel¹
for the INSIGHT-preAD study group
and the Alzheimer Precision Medicine Initiative (APMI)

- (1) Sorbonne University, GRC n° 21, Alzheimer Precision Medicine (APM), AP-HP, Pitié-Salpêtrière Hospital, Boulevard de l'hôpital, F-75013, Paris, France
- (2) Brain & Spine Institute (ICM), INSERM U 1127, CNRS UMR 7225, Boulevard de l'hôpital, F-75013, Paris, France
- (3) Institute of Memory and Alzheimer's Disease (IM2A), Department of Neurology, Pitié-Salpêtrière Hospital, AP-HP, Boulevard de l'hôpital, F-75013, Paris, France
- (4) Institute of Neuroscience and Physiology, Department of Psychiatry and Neurochemistry, The Sahlgrenska Academy at the University of Gothenburg, Mölndal, Sweden
- (5) Clinical Neurochemistry Laboratory, Sahlgrenska University Hospital, Mölndal, Sweden
- (6) Department of Neurodegenerative Disease, UCL Institute of Neurology, Queen Square, London, UK
- (7) UK Dementia Research Institute, London, UK
- (8) ICM Institut du Cerveau et de la Moelle épinière, CNRS UMR7225, INSERM U1127, UPMC, Hôpital de la Pitié-Salpêtrière, 47 Bd de l'Hôpital, F-75013 Paris, France
- (9) Sorbonne Université, CNRS, INSERM, Laboratoire d'Imagerie Biomédicale, F-75013, Paris, France
- (10) Centre pour l'Acquisition et le Traitement des Images (www.cati-neuroimaging.com), France
- (11) AP-HP, Hôpital Pitié-Salpêtrière, Département de Médecine Nucléaire, F-75013, Paris, France
- (12) Department of Clinical and Experimental Medicine, University of Pisa, Pisa, Italy
- (13) Department of Drug Sciences, University of Catania, Catania, Italy
- (14) Oasi Research Institute - IRCCS, Troina, Italy

*** Correspondence to:**

Andrea Vergallo, MD

Sorbonne University Clinical Research Group (GRC n°21)

“Alzheimer Precision Medicine (APM)”

Établissements Publics à caractère Scientifique et Technologique (E.P.S.T.)

Alzheimer Precision Medicine Initiative (APMI)

<https://www.apmiscience.com/>

Phone: +33 1 57 27 46 74

Fax: +33 1 57 27 46 74

E-Mail: a_vergallo@yahoo.com; andrea.vergallo@icm-institute.org

§ Both authors contributed equally to this work

Running Title: Plasma YKL-40 in the INSIGHT-preAD study.

Abstract

Neuroinflammation, a key early pathomechanistic alteration of Alzheimer's disease (AD), may represent either a detrimental or a compensatory mechanism or both (according to the disease stage).

YKL-40, a glycoprotein highly expressed in differentiated glial cells, is a candidate biomarker for *in-vivo* tracking neuroinflammation in humans.

We performed a longitudinal study in a mono-centric cohort of cognitively healthy individuals at risk for AD exploring whether age, sex, and the Apolipoprotein E $\epsilon 4$ allele affect plasma YKL-40 concentrations. We investigated whether YKL-40 is associated with brain amyloid- β ($A\beta$) deposition, neuronal activity, and neurodegeneration as assessed *via* neuroimaging biomarkers. Lastly, we investigated whether YKL-40 may predict the cognitive performance.

We found an age-associated increase of YKL-40 and observed that men display higher concentrations than women, indicating a potential sexual dimorphism.

Moreover, YKL-40 was positively associated with memory performance and negatively associated with brain $A\beta$ deposition (but not with metabolic signal). Consistent with translational studies, our results suggest a potentially protective effect of glia on incipient brain $A\beta$ accumulation and neuronal homeostasis.

Key words: Alzheimer's disease; neuroinflammation; YKL-40; sex; amyloid.

Abbreviations: $A\beta$ = amyloid beta; APMI = Alzheimer Precision Medicine Initiative; APMI-CP = Alzheimer Precision Medicine Initiative Cohort Program; *APOE* $\epsilon 4$ = Apolipoprotein $\epsilon 4$ allele; BF = basal forebrain; ^{18}F -FDG-PET = ^{18}F -fluorodeoxyglucose-PET; HP = hippocampal; LMM = linear mixed model; MCI = mild cognitive impairment; SD =

standard deviation; SMC = subjective memory complaint; SUVR = standardized uptake value ratio; TGF- β 1 = transforming-growth-factor- β 1; TIV = total intracranial volume.

INTRODUCTION

Experimental models of Alzheimer's disease, as well as *in-human* neuropathological studies, indicate that the dysregulation of the CNS immune surveillance and the over-amplification of inflammatory responses (i.e., neuroinflammation) represents one of the earliest pathomechanistic alterations of Alzheimer's disease (Arranz and De Strooper, 2019; Edwards, 2019; Heneka et al., 2015; Heppner et al., 2015; Rawji et al., 2016).

Neuroinflammation is associated with toxic accumulation of amyloid- β ($A\beta$) and tau protein, synaptic dysfunction, and neurodegeneration (Arranz and De Strooper, 2019; Edwards, 2019; Heneka et al., 2015; Shi and Holtzman, 2018).

However, it is not **entirely** known whether neuroinflammation may represent either a detrimental mechanism or a compensatory dynamic or both (according to the disease stage) with regard to $A\beta$ accumulation, synaptic dysfunction, neurodegeneration and cognitive performance in subjects at risk for Alzheimer's disease (Arranz and De Strooper, 2019; Edwards, 2019; Heneka et al., 2015; Shi and Holtzman, 2018). In addition, the **critical** biological factors influencing neuroinflammation in humans have not extensively been investigated in subjects at risk for Alzheimer's disease.

In Alzheimer's disease, reactive glial cells co-localize with brain $A\beta$ deposits indicating a central role of $A\beta$ pathophysiology in triggering and sustaining neuroinflammation (Edwards, 2019; Hampel et al., 2019a; Heneka et al., 2015; Heppner et al., 2015). In addition, suppression of the expression of some protective genes expression, inhibition of key regulatory proteins, and glial senescence are all associated with increased $A\beta$ plaques seeding, loss of synaptic homeostasis, and neurodegeneration indicating a crucial protective role of glial cells regarding key physiological brain functions (Arranz & De Strooper, 2019; Shi & Holtzman, 2018).

All this robust and increasing evidence has pointed out neuroinflammation as a prime therapeutic target for pathway-based targeted strategies with a disease-modifying effect.

However, the temporal and spatial dynamics among neuroinflammation and other **core** pathophysiological mechanisms of Alzheimer's disease are poorly understood. **Moreover**, whether glia cells may play a compensatory or a detrimental role or both, according to the disease stage, needs to be elucidated.

Whether neuroinflammation, like other Alzheimer's disease pathophysiological processes, display sex-based differences, should also be elucidated to inform pharmacological research. In this regard, experimental evidence suggests the presence of sexual dimorphism in brain immune and inflammatory responses (Acáz-Fonseca et al., 2015; Rawji et al., 2016; Santos-Galindo et al., 2011; Schwarz and McCarthy, 2008; VanRyzin et al., 2018; Vest and Pike, 2013).

To address all scientific questions, biomarkers-based investigations are needed to generate new insights and potentially orientate **future** drug-biomarker co-development pipelines targeting neuroinflammation.

YKL-40 (or chitinase 3-like protein 1 [CHI3L1]) – a chitinase-like glycoprotein belonging to the glycosyl hydrolase family 18 (Alcolea et al., 2014; Baldacci et al., 2019; Molinuevo et al., 2018) – is one of the **most robust** neuroinflammatory candidate biomarkers. It is supposed to track human macrophage differentiation expressed in glial cells (Baldacci et al., 2019; Bonneh-Barkay et al., 2012). The physiological role and specific cell surface receptor are not known; however, YKL-40 has been hypothesized to be involved in tissue remodeling during inflammation (Baldacci et al., 2019; Bonneh-Barkay et al., 2012).

Accumulating evidence supports the utilization of CSF YKL-40 concentrations since they can: 1) distinguish patients with Alzheimer's disease dementia from cognitively **healthy** controls (Choi et al., 2011; Craig-Schapiro et al., 2010; Kester et al., 2015; Lleo et al., 2019;

Olsson et al., 2016), 2) predict the progression of cognitive decline from preclinical/prodromal Alzheimer's disease / mild cognitive impairment (MCI) to Alzheimer's disease dementia, and 3) be associated with biomarkers of Alzheimer's disease pathophysiological mechanisms, including brain proteinopathies, synaptic dysfunction, axonal damage and neurodegeneration (Alcolea et al., 2015; Antonell et al., 2014; Falcon et al., 2019; Gispert et al., 2016; K. Hellwig et al., 2015).

Most of the studies focusing on YKL-40 have chiefly been confined to the CSF matrix. However, plasma concentrations of YKL-40 have already been demonstrated to robustly correlate with the corresponding CSF concentrations (Craig-Schapiro et al., 2010; Pierscianek et al., 2019; Zhang et al., 2019). In particular, Craig-Shapiro and colleagues investigated CSF YKL-40 as a prognostic marker in preclinical AD and reported a positive correlation between CSF and blood concentrations of the candidate marker ($r=0.237$; $p=0.0002$) (Craig-Schapiro et al., 2010). Zhang and colleagues investigated YKL-40 in treatment resistant epileptic patients and showed a positive correlation between blood and CSF concentrations of YKL-40 ($r >0.70$ and $p <0.001$, across study groups) (Zhang et al., 2019).

In the present study, we investigated the cross-sectional and longitudinal impact of primary biological factors – namely age, sex, and the Apolipoprotein E (*APOE*) $\epsilon 4$ allele – on neuroinflammation in terms of YKL-40 plasma concentrations. To follow, we explored the cross-sectional and longitudinal association of plasma YKL-40 concentrations with 1) brain $A\beta$ deposition – assessed using $A\beta$ -PET, 2) rates of cortical metabolic activity, a proxy for neuronal activity – assessed through ^{18}F -fluorodeoxyglucose-PET (^{18}F -FDG-PET), and 3) brain volumes typically affected in early Alzheimer's disease using MRI, i.e., hippocampal (HP) entorhinal cortex, and basal forebrain (BF) volumes. Lastly, we carried out an exploratory association study between YKL-40 and neurocognitive scores. The present study was performed in a mono-centric cohort of cognitively healthy individuals with subjective

memory complaint (SMC), a condition at risk for Alzheimer's disease (Buckley et al., 2016; Dubois et al., 2018; van Harten et al., 2018).

MATERIALS AND METHODS

Study participants

The study participants were enrolled in the standardized, large-scale, observational, monocentric, French academic university-based “INveStIGATION of AlzHeimer's PredicTors in Subjective Memory Complainers” (INSIGHT-preAD) study (Dubois et al., 2018) – which is part of the Alzheimer Precision Medicine Initiative (APMI) and its established Cohort Program (APMI-CP) (Hampel et al., 2019b, 2018a, 2018b). Participants were enrolled at the Institute of Memory and Alzheimer's disease (*Institut de la Mémoire et de la Maladie d'Alzheimer*, IM2A) at the Pitié-Salpêtrière University Hospital in Paris, France.

The main objective of the INSIGHT-preAD study is to explore the earliest preclinical stages of Alzheimer's disease through intermediate to later stages until progression to conversion to first cognitive symptoms, using comprehensive clinical parameters and biomarkers associated with cognitive decline.

The INSIGHT-preAD study includes 318 cognitively and physically normal Caucasian individuals, recruited from the community in the wider Paris area, France, aged 70 to 85, with SMC. The status of SMC was confirmed as follows: (i) participants gave an affirmative answer (“YES”) to both questions: “Are you complaining about your memory?” and “Is it a regular complaint that has lasted for more than 6 months?”; (ii) participants showed intact cognitive functions based on the Mini-Mental State Examination score (MMSE, ≥ 27), Clinical Dementia Rating scale (CDR = 0), and Free and Cued Selective Rating Test (FCSRT, total recall score ≥ 41). A β -PET investigation was performed at baseline visit, as mandatory inclusion criterion. Thus, all subjects enrolled into the study have SMC and are stratified as

either positive or negative for cerebral A β deposition. At the point of the study inclusion, several data were collected, namely demographic and clinical data, and Apolipoprotein E (APOE) genotype (see Supplementary materials for more details). Exclusion criteria were: a history of neurological or psychiatric diseases, including depressive disorders.

The study was conducted in accordance with the tenets of the Declaration of Helsinki of 1975 and approved by the local Institutional Review Board at the participating center (Ethical approval number: 2013-Fev-13150). All participants or their representatives gave written informed consent for the use of their clinical data for research purposes.

Blood sampling and immunoassays

Ten (10) mL of venous blood were collected in one BD Vacutainer® tube (lithium heparin), which was employed for all subsequent immunological analyses. Blood samples were taken in the morning, after a 12-hour fast, handled in a standardized way, and centrifuged for 15 minutes at 2,000 G-force at 4°C. Per sample, plasma fraction was collected, homogenized, aliquoted into multiple 0.5 mL cryovial-sterilized tubes, and finally stored at –80°C within 2 hours from collection.

Longitudinal data for plasma concentrations of YKL-40 were collected across three time-points, beginning at participants' enrollment ("baseline visit" or "M0") over a three-year follow-up (one-year follow-up or "M12" and three-year follow-up or "M36").

Immunoassay for plasma YKL-40

Plasma YKL-40 concentration was measured using a commercially available ELISA kit (R&D Systems, Minneapolis, MN, US), according to manufacturer's instructions. Repeatability was 6.6% and 6.9% and intermediate precision 6.6% and 6.9%, for two internal quality control plasma samples with concentrations of 14.1 pg/mL and 108.0 pg/mL. All

samples were analyzed using one batch of reagents by board-certified laboratory technicians who were blinded to clinical data (Vergallo et al., 2019).

PET data acquisition and processing

A β and ^{18}F -FDG-PET investigations were performed at the baseline visit (“M0”) – as mandatory inclusion criterion – and at two-year follow-up (“M24”).

Brain **A β -PET** scans were acquired 50 minutes after injection of 370 MBq (10 mCi) of ^{18}F -Florbetapir, which has high affinity for amyloid plaques. Brain ^{18}F -FDG scans were obtained 30 minutes after injection of 2 MBq/kg of 2-deoxy-2-(^{18}F)fluoro-D-glucose (^{18}F -FDG). All acquisitions were performed in a single session on a Philips Gemini GXL scanner and consisted of 3 x 5 minutes frames with a voxel size of 2 x 2 x 2 mm³. Images were then reconstructed using iterative LOR-RAMLA algorithm (10 iterations), with a “smooth” post-reconstruction filter. All corrections (attenuation, scatter and random coincidence) were integrated into the reconstruction. Lastly, frames were realigned, averaged, and quality-checked by the CATI team (*Centre d'Acquisition et Traitement des Images*). CATI is a French neuroimaging platform (available at <http://cati-neuroimaging.com>) (Dubois et al., 2018).

Reconstructed PET images are analyzed with a pipeline developed by the CATI team, according to a method previously described (Dubois et al., 2018; Habert et al., 2018).

Standard uptake value ratios (SUVR) were calculated for each of 12 bilateral cortical regions of interest (anterior and posterior cingulate, superior frontal, inferior parietal, middle temporal cortices, and precuneus), as well as the global average SUVR. **The pons and whole cerebellum regions were used as reference for individual voxel normalization in the partial volume effect corrected images (see Supplementary material for more details).**

¹⁸F-FDG-PET scans were assessed in a separate session. Cortical metabolic indices were calculated in the bilateral anterior cingulate cortex, posterior cingulate cortex, inferior parietal lobe, precuneus, middle temporal cortex, and hippocampus, and the pons was used as the reference region.

MRI acquisitions and processing

Brain **structural** MRI acquisitions were conducted using a 3 Tesla MRI scanner (Siemens Magnetom Verio, Siemens Medical Solutions, Erlangen, Germany). Details regarding the 3D-T1 magnetic resonance imaging protocols of acquisition are reported in the **Supplementary material**. **At the moment the present study was performed, MRI was available at M0 and M24.**

HP, entorhinal, and BF volumes

For the automated calculation of individual HP and BF volumes, the 3D-T1 MRI data were processed using statistical parametric mapping (SPM8, Wellcome Trust Center for Neuroimaging) and the VBM8 toolbox (available at <http://dbm.neuro.uni-jena.de/vbm>). EC volume was defined using the probabilistic maps present in the SPM Anatomy Toolbox. The technical details of these procedures are described in the **Supplementary material**. The delineation of the HP follows the consensual standard space harmonized protocol labels as described in detail by Wolf and colleagues (Wolf et al., 2017). Modulated white matter voxel values were included in the HP volume calculation because the harmonized protocol explicitly specifies to include small white matter regions (alveus and fimbria) in HP segmentation (Cavedo et al., 2018). The delineation and localization of the cholinergic BF followed the Mesulam's nomenclature based on the histological serial coronal sections and postmortem MRI scan of a brain from a 56-year-old man, as previously described (Cavedo et

al., 2018). HP and BF volumes were corrected to the total intracranial volume (TIV) using the residuals method.

First, a linear regression of the volume of a neuroanatomical structure on the TIV was fitted to the entire dataset. From the fitted model, the residuals, which are differences between actual volume and fitted volume based on a subject's TIV, were calculated (Cavedo et al., 2018). The TIV-corrected measurements were expressed as $Vol_adji = Vol_i - b (TIV_i - \text{meanTIV})$ (Cavedo et al., 2018). Vol_adji is the TIV-adjusted volume of the subject i , Vol_i is the original uncorrected volume of the subject i , b is the slope from the linear regression of Vol on TIV , TIV_i is the TIV for the subject i , and meanTIV is the mean TIV across all subjects.

STATISTICAL ANALYSIS

The analyses were performed excluding those individuals without YKL-40 concentrations at baseline, leading to a sample of 314 participants. In order to have a normal distribution, we used the natural logarithm of YKL-40 plasma concentration.

First, we studied the univariate association between plasma YKL-40 concentrations and age, sex, and *APOE* $\epsilon 4$ allele. Linear models (LM) were used for baseline exploration and linear mixed models (LMM) for longitudinal analysis over a three-year follow-up (M0, M12, and M36).

To investigate the effect of the variable of interest on longitudinal changes of YKL-40, LMM with a random intercept were built including a time interaction. LMM is especially suitable for repeated measures with a considerable number of missing data across time points and to confirm neuroimaging baseline data calculated with a longitudinal pipeline. Indeed, the strength of this model is to focus on subject trajectories considering the correlation between

time-points, thus allowing intra- and inter-individual comparisons, although the number of subjects decreases over time (Edwards, 2000; Twisk et al., 2013).

To follow, we investigate the effect of baseline YKL-40 concentration on imaging data at baseline and over a two-year follow-up (M0 and M24). Baseline investigations were conducted using LM adjusted on age, sex, and *APOE* $\epsilon 4$ carrier status. The longitudinal investigation was conducted using LMM with random intercept using the same covariates in addition to time and time*YKL-40 interaction. This interaction was used to investigate the effect of baseline YKL-40 concentration on longitudinal changes in imaging data.

The association between baseline YKL-40 concentration and A β -PET outcome measures was assessed in terms of baseline and longitudinal SUVRs (both global and regional). Then, we tested the association between baseline YKL-40 concentration and both baseline and longitudinal ^{18}F -FDG-PET regionally. Likewise, the association between YKL-40 concentration and MRI volume was assessed both at baseline and longitudinally.

We also investigated the effect of baseline YKL-40 on cognitive measures at baseline and over a 3-year follow-up (M0, M12, M24, and M36). LMM was adjusted age, sex, and *APOE* $\epsilon 4$ carrier status. The longitudinal investigation was conducted using LMM with random intercept and slope using the same covariates in addition to time and time*YKL-40 interaction. This interaction was used to investigate the effect of baseline YKL-40 concentration on longitudinal changes in cognitive performances. Because of non-normal distribution, Mini-Mental State Examination (MMSE) and Free and Cued Selective Reminding Test (FCSRT) were analyzed using binomial models instead of linear models.

Finally, we investigated the effect of 1-year changes of YKL-40 concentration on imaging and cognitive data at M24 and over 2-years changes using linear model adjusted on age, sex, and *APOE* $\epsilon 4$ carrier status. **We used deltas for the calculation of the 1-year changes of YKL-40 and the 2-years changes of imaging and cognitive measures.**

Normality of residuals was visually checked for each model. Statistical significance of parameters was determined testing for the nullity of the estimators computed by the models. For LMM only, the degrees of freedom were determined according to the Satterthwaite approximation (Luke, 2017; SATTERTHWAITE, 1946). *P* values < 0.05 were considered significant in all statistical elaboration. We then performed adjustment of significance for multiple comparisons using False Discovery Rate (FDR) correction whenever appropriate.

For cross-sectional and longitudinal analysis, Cohen's f^2 were calculated to assess effect sizes. Statistical analyses were performed using R software, version 3.6.0, including the libraries “lme4” and “lmerTest”, both available at <http://cran.r-project.org/web/packages>.

Data availability

Anonymized data not published within this article will be made available by request from any qualified investigator after evaluation of the request by the INSIGHT-preAD Scientific Committee.

RESULTS

Sociodemographic features, *APOE* $\epsilon 4$ allele frequencies, and plasma concentrations of YKL-40 at baseline, in the INSIGHT-preAD cohort are presented for each time point in **Table 1**. The number of subjects with available data of plasma YKL-40, at each time point, is 314 (at baseline), 227 (at one-year follow-up), 131 (at three-year follow-up). Longitudinal data on neuroimaging and cognitive variables are reported in Supplementary Tables 1, 2, and 3.

Men display higher YKL-40 concentrations than women

We found significantly higher YKL-40 concentrations in men compared to women, at baseline ($b=0.151$, **Cohen's $f^2=0.014$** , $P=0.036$, adjusted $P=0.054$; see also **Table 2** and **Fig. 1**) and, as shown by the LMM analysis, at each time-point ($b=0.171$, **Cohen's $f^2=0.017$** , $P=0.015$, adjusted $P=0.023$). However, no significant two-way interaction of time and sex on YKL-40 was found (see also **Table 2** and **Fig. 2**). Hence, a sexual dimorphism in plasma YKL-40 concentrations was found, across the time-points investigated, in our cohort of SMC individuals.

Baseline age impacts YKL-40 concentrations

We found a significantly positive association between plasma YKL-40 concentrations and age at baseline ($b=0.028$, **Cohen's $f^2=0.027$** , $P=0.004$, adjusted $P=0.012$; see also **Table 2**). We further explored the effect of age at baseline on YKL-40 concentrations across the three-year follow-up. The LMM confirmed the **association with** age at each time-point ($b=0.029$, **Cohen's $f^2=0.027$** , $P=0.003$, adjusted $P=0.009$) but did not show an interaction of time and age (see also **Table 2** and **Fig. 3**). These results suggest that age is a factor potentially influencing pathophysiological processes tracked by our candidate biomarker.

No effect of *APOE* $\epsilon 4$ allele on plasma YKL-40 concentrations

We did not observe a significant effect of *APOE* $\epsilon 4$ allele on baseline plasma YKL-40 concentration nor over a three-year follow-up (see **Table 2**).

Effect of plasma YKL-40 concentrations on the rate of brain A β deposition

We investigated whether baseline plasma YKL-40 concentrations are associated with baseline and longitudinal changes of brain A β deposition at both the global and regional levels.

We found a significantly negative correlation between plasma YKL-40 concentrations and baseline global A β -PET SUVR ($b=-0.025$, Cohen's $f^2=0.015$, $P=0.036$; see also **Fig. 4**). Plasma YKL-40 concentrations were associated with A β -PET SUVR in the left and right superior orbitofrontal cortex ($b=-0.029$, Cohen's $f^2=0.019$, $P=0.018$ and $b=-0.028$, Cohen's $f^2=0.017$, $P=0.025$, respectively) and in left and right inferior parietal cortex ($b=-0.029$, Cohen's $f^2=0.019$, $P=0.019$ and $b=-0.030$, Cohen's $f^2=0.018$, $P=0.022$, respectively), however no significant result survived the correction for multiple comparisons (see also **Table 3**).

LMM confirmed the negative association between YKL-40 concentrations and global A β -PET SUVR, at M0 ($b=-0.025$, Cohen's $f^2=0.015$, $P=0.047$). LMM also showed a negative association, at M0, between plasma YKL-40 concentrations and A β -PET SUVR in the following regions: left and right superior orbitofrontal cortex ($b=-0.028$, Cohen's $f^2=0.013$, $P=0.028$ and $b=-0.027$, Cohen's $f^2=0.016$, $P=0.039$, respectively), and left and right inferior parietal cortex ($b=-0.028$, Cohen's $f^2=0.015$, $P=0.032$ and $b=-0.029$, Cohen's $f^2=0.016$, $P=0.028$, respectively), see also **Table 3**.

However, no association was found between YKL-40 and longitudinal changes of A β -PET SUVR, either global or regional. No effect of 1-year changes of YKL-40 concentration was found on A β -PET SUVR at M24 or over 2-year changes (see **Supplementary Table 4**).

No effect of plasma YKL-40 concentrations on ^{18}F -FDG-PET and brain volumes

We investigated whether baseline plasma YKL-40 concentrations are associated with baseline and longitudinal **rates of brain glucose consumption, widely considered a surrogate marker of synaptic activity**. The cross-sectional and longitudinal analysis did not show a significant association between YKL-40 concentrations and regional ^{18}F -FDG-PET (see

Table 5). No association between 1-year changes of YKL-40 concentration and ^{18}F -FDG-PET at M24 or over 2-years changes was found (see **Supplementary Table 6**).

We did not find any significant effect of YKL-40 on HP, BF, or entorhinal cortex volume at M0 or M24. Neither a significant interaction between time and YKL-40 on brain volumes was found (see **Supplementary Table 7**). Moreover, we did not observe any association between 1-year changes of YKL-40 concentration and MRI volume at M24 or over 2-years changes (see **Supplementary Table 8**).

Longitudinal effect of plasma YKL-40 on memory performance

We found that an increase of YKL-40 concentration over 1 year was positively associated with a higher FCSRT total recall score at M24 ($b=0.308$, **Cohen's $f^2=0.005$** , $P=0.023$; see also see **Table 4 and Fig. 5**).

We did not find any significant effect of YKL-40 on MMSE, FCSRT, verbal fluency, Trail Making Test scores at each time point investigated (M0, M12, and M24). No significant interaction between time and YKL-40 on cognitive performance was detected (see **Supplementary Table 9**).

DISCUSSION

We found that higher concentrations of YKL-40 were associated **with male sex**, lower overall and regional cross-sectional $\text{A}\beta$ deposition as well as higher memory scores over time.

Taken together, all these results suggest no clinical detrimental effect / potential protective effect of glia activation, as reflected by the candidate biomarker, in our cohort of cognitively healthy individuals at risk for Alzheimer's disease.

Although significant these association shows a very small effect size; thus, any hypothesis we here draw needs to be approached cautiously.

Sex effect on plasma YKL-40 concentrations

We provide the first longitudinal *in-vivo* demonstration of a potential sex effect on glial activation, in terms of plasma YKL-40 concentrations, in a cohort of cognitively healthy individuals at risk for Alzheimer's disease.

Our results are in line with **existing** literature pointing out a sexual dimorphism in inflammation and immune response.

Recent *in-vitro* and animal models of neuroinflammation show a higher reactivity of glial cells, especially astrocytes, in males subjects compared with females. Astrocytes express enzymes involved in steroid synthesis and metabolism and may express higher levels of interleukin-6, tumor necrosis factor- α , and interleukin-1 β (all **hypothesized** to be upregulated in both aging and Alzheimer's disease) under androgen stimulation rather than estrogens stimulation (Santos-Galindo et al., 2011). Moreover, although astrocytes display the same basal levels of pro-inflammatory mediators across sexes, males seem to develop a more intense inflammatory response under stress conditions (Acaz-Fonseca et al., 2015; Santos-Galindo et al., 2011). **By contrast**, estradiol has a greater effect than androgens in suppressing the extracellular signal-regulated kinase1/2 signaling pathway, decreasing cell proliferation, and stimulating apoptotic pathways in astrocytes (Zhang et al., 2002). Rodent models of neuroinflammation exhibit sexual dimorphism in microglia-driven neuroinflammatory

responses, with males showing higher inflammatory reactivity than females (Villa et al., 2018).

We acknowledge that our inter-sex differences in plasma YKL-40 concentrations contradicts previous CSF-based investigations that did not report any sex-based difference in term of YKL-40 concentrations or reported higher levels of the marker in females (Craig-Schapiro et al., 2010; Grewal et al., 2016; Janelidze et al., 2018). It would be essential to assess whether the sex-biased difference in body fluids YKL-40 is influenced by the sex differences in glial cells count (McCarthy et al., 2017).

If our study was corroborated, next clinical trials targeting neuroinflammation **should take into account** sex-biased biological and functional outcomes. Moreover, sex-related outcome analyses and comparative active-treatment dose-finding substudies may be recommended.

Effect of age on plasma YKL-40 concentrations

We found that age impacts YKL-40 concentrations regardless of the time point investigated. An effect of age on CSF YKL-40 has already been reported. These findings are consistent with the well-established aging-effect on immunosenescence, immunosurveillance, and thus neuroinflammation (Hempel et al., 2019a). In addition, an age-related regional synaptic vulnerability, driven by aberrant microglia, has been reported (Graham et al., 2019; Guerra-Gomes et al., 2017).

Effect of APOE $\epsilon 4$ allele on plasma YKL-40 concentrations

Like previous CSF-based studies (Baldacci et al., 2017; Craig-Schapiro et al., 2010), we did not find any effect of APOE $\epsilon 4$ allele on YKL-40 concentrations. Experimental models of

Alzheimer's disease showed that *APOE* deficiency, a condition that reflects the *APOE* $\epsilon 4$ allele carrier status, is associated with attenuated inflammation (Kim et al., 2011; Shin et al., 2014). For instance, Shy and colleagues reported that the genetic ablation of *APOE* significantly slows down both activation of glial cells and neuronal loss (Shi et al., 2017). Despite a role of *APOE* $\epsilon 4$ allele in neuroinflammatory processes stands out of genetic studies (Arranz and De Strooper, 2019; Shi and Holtzman, 2018), the molecular dynamics whereby *APOE* $\epsilon 4$ allele may trigger or facilitate neuroinflammation in Alzheimer's disease are not clear.

It is conceivable that the overall effect of the *APOE* gene may be explained in light of the APOE-TREM2 protein interaction (Krasemann et al., 2017).

*Association of plasma YKL-40 concentrations with the cerebral **accumulation** of A β*

We found a negative association between plasma YKL-40 and the cerebral **level** of A β , as assessed through global A β -PET SUVR. This result aligns with the robust body of translational studies indicating a potential compensatory role of glia during incipient brain amyloidosis in Alzheimer's disease. Indeed, rodent models of Alzheimer's disease indicated the ability of astrocytes to uptake and clear A β in subjects bearing cerebral fibrillar aggregates and diffuse plaques (Gomez-Arboledas et al., 2018; Perez-Nievas and Serrano-Pozo, 2018; Pihlaja et al., 2008; Serrano-Pozo et al., 2013). **By contrast**, the shutdown of astrocyte-mediated homeodynamics is associated with increased A β plaque burden and synaptic terminals dystrophy. Therefore, it seems that a contribution of astrocytes and microglia in ensuring A β homeostasis occurs with the reactive gliosis commences or increases as A β monomers start aggregating into oligomers and then fibrils (De Strooper and Karran, 2016; Oide et al., 2006; Wyss-Coray et al., 2003). **It has been hypothesized that an increased astrocyte phagocytic activity may represent a compensatory mechanism to counteract**

incipient A β overaccumulation and prevent neurotoxicity induced by A β species (De Strooper and Karran, 2016; Oide et al., 2006; Wyss-Coray et al., 2003).

Regarding microglia, experimental models of Alzheimer's disease point out it may contribute both in A β clearance and in limiting the growth and further accumulation plaques (Edwards, 2019; S. Hellwig et al., 2015; Zhao et al., 2017). In addition, the dysregulation of microglia activity, including dystrophic microglia, may be either a trigger or a worsening factor, or both, of the seeding of aberrant protein aggregates in the brain (Edwards, 2019; Streit et al., 2009).

We also report a significantly negative association between plasma YKL-40 concentrations and the regional levels of A β . While only some trends survive the correction for multiple comparisons, we all the due caution, we here provide an interpretation of our results. All significant regions belong to the default mode network (DMN), one of the earliest network displaying A β deposition in preclinical stages of Alzheimer's disease.

The non-detrimental (and potentially protective role) that neuroinflammation may play in our individuals is further supported by the fact that we did not find any association between YKL-40 concentrations and the following outcomes: 1) neuronal activity 2) brain volumes, 3) cognitive performance. In addition, we found a positive association between 1-year changes of YKL-40 and memory performance over 2 years. Two alternative versions of FCSRT, were used from one visit to the next, to minimize repetition effects (Gagliardi et al., 2019); however, studies with longer follow-up should be carried out to corroborate such finding that holds considerable clinical potential.

Thus, we argue that the lack of any significant association between YKL-40 and neuroimaging outcomes coupled with the significant negative association between YKL-40 and A β -PET SUVRs, as well as the positive longitudinal association between the former and

memory performance, support the hypothesis of a compensatory and not detrimental role of neuroinflammation in our cohort of cognitively healthy individuals.

Limitations

The present study has some potential caveats that need to be addressed. The relatively small size of individuals longitudinally assessed with plasma YKL-40 measurement might have biased the longitudinal results.

In addition, the low number of converters – both SMC to MCI and overt dementia does not allow reaching any meaningful biological or clinical conclusion on the role of plasma YKL-40 in predicting pathophysiological or cognitive trajectories in cognitively normal individuals at risk of Alzheimer's disease (see **Supplementary Fig. 1** for more details).

In this regard, we have planned the extension of the clinical, neuroimaging, and biological follow-up of the INSIGHT-preAD study to assess whether distinct longitudinal trajectories of plasma YKL-40 may predict synaptic dysfunction and neurodegeneration as well as the development of objective cognitive impairment. This extended study design will also help understand whether plasma YKL-40 concentrations may represent a diagnostic, prognostic, or predictive biomarker.

The nature of our study is exploratory, given the fact that this is the first study ever employing plasma YKL-40 concentrations in a cohort of cognitively healthy individuals at risk for Alzheimer's. For this reason, we decided to use a broad set of multimodal biomarkers taking the risk that some significant results may neither survive adjustment for multiple comparisons nor be strong enough to reach definitive clinical conclusions. After the correction for multiple comparisons, all the most important significant effects remain, whereas some of the associations between plasma YKL-40 concentrations and regional A β -PET SUVR vanish, and only a trend toward significance is present.

Moreover, most of the significant associations here reported display very small effect sizes, which call for a corroboration study and make our argumentation speculative.

We do believe that a study with a larger sample would increase the power of the statistical analysis and would likely lead to a stronger statistical significance.

Given the low number of A β -PET positive individuals, at both baseline and follow-up, we decided not to investigate the association between our candidate biomarker and A β -PET SUVR in the A β -PET-based groups. Beyond mere statistical power issues, we also set out not to focus on PET-based “diagnostic” categories but rather to explore the association between levels of brain amyloid and our candidate marker. Thresholds for A β -PET may substantially vary across cohorts, especially in preclinical populations, and so results related to A β -PET positivity *versus* negativity may do.

Finally, potential influences of genetic polymorphisms other than *APOE* $\epsilon 4$ allele, including but not exclusively the TREM2 variant, on modifications of plasma YKL-40 concentrations should be investigated.

CONCLUSIONS

Growing evidence points to a crucial and upstream role of both immune and proinflammatory mechanisms in the pathophysiology of neurodegenerative diseases, including Alzheimer’s disease.

Exploring the interaction between YKL-40 and Alzheimer’s disease pathophysiological hallmarks can help elucidate the mechanisms underlying the complex dynamic among A β dysmetabolism, neuronal activity, and neuroinflammation. Consequently, neuroinflammatory

phenotypes could be better categorized, thus influencing the progress in the evolving area of neuroinflammatory clinical trials.

In this regard, plasma YKL-40 may represent a robust and reliable tool to enrich clinical trials investigating compounds with a putative disease-modifying effect.

Acknowledgments

The research and this manuscript was part of the translational research program “**PHOENIX**”, awarded to HH, and administered by the Sorbonne University Foundation and sponsored by la *Fondation pour la Recherche sur Alzheimer*.

The study was promoted by INSERM in collaboration with ICM, IHU-A-ICM and Pfizer and has received support within the "Investissement d'Avenir" (ANR-10-AIHU-06) French program. The study was promoted in collaboration with the "CHU de Bordeaux" (coordination CIC EC7), the promoter of Memento cohort, funded by the Foundation Plan-Alzheimer. The study was further supported by AVID/Lilly.

CATI is a French neuroimaging platform funded by the French Plan Alzheimer (available at <http://cati-neuroimaging.com>).

INSIGHT-preAD Study Group:

Hovagim Bakardjian, Habib Benali, Hugo Bertin, Joel Bonheur, Laurie Boukadida, Nadia Boukerrou, Enrica Cavedo, Patrizia Chiesa, Olivier Colliot, Bruno Dubois, Marion Dubois, Stéphane Epelbaum, Geoffroy Gagliardi, Remy Genthon, Marie-Odile Habert, Harald Hampel, Marion Houot, Aurélie Kas, Foudil Lamari, Marcel Levy, Simone Lista, Christiane Metzinger, Fanny Mochel, Francis Nyasse, Catherine Poisson, Marie-Claude Potier, Marie Revillon, Antonio Santos, Katia Santos Andrade, Marine Sole, Mohamed Surtee, Michel Thiebaut de Schotten, Andrea Vergallo, Nadjia Younsi.

AV is an employee of Eisai Inc. This work has been performed during his previous position at Sorbonne University, Paris, France.

HZ is a Wallenberg Academy Fellow supported by grants from the Swedish Research Council (#2018-02532), the European Research Council (#681712) and Swedish State Support for Clinical Research (#ALFGBG-720931), as well as the UK Dementia Research Institute at UCL.

KB holds the Torsten Söderberg Professorship of Medicine and is supported by the Swedish Research Council (#2017-00915), the Swedish Alzheimer Foundation (#AF-742881), Hjärnfonden, Sweden (#FO2017-0243), and a grant (#ALFGBG-715986) from the Swedish state under the agreement between the Swedish government and the County Councils, the ALF-agreement.

HH is an employee of Eisai Inc. This work has been performed during his previous position at Sorbonne University, Paris, France. At Sorbonne University he was supported by the AXA Research Fund, the “*Fondation partenariale Sorbonne Université*” and the “*Fondation pour la Recherche sur Alzheimer*”, Paris, France.

Contributors to the Alzheimer Precision Medicine Initiative – Working Group (APMI-WG):

Mohammad AFSHAR (France), Lisi Flores AGUILAR (Canada), Leyla AKMAN-ANDERSON (USA), Joaquín ARENAS (Spain), Jesús ÁVILA (Spain), Claudio BABILONI (Italy), Filippo BALDACCI (Italy), Richard BATRLA (Switzerland), Norbert BENDA (Germany), Keith L. BLACK (USA), Arun L.W. BOKDE (Ireland), Ubaldo BONUCCELLI (Italy), Karl BROICH (Germany), Francesco CACCIOLA (Italy), Filippo CARACI (Italy), Giuseppe CARUSO (Italy), Juan CASTRILLO† (Spain), Enrica CAVEDO (France), Roberto CERAVOLO (Italy), Patrizia A. CHIESA (France), Massimo CORBO (Italy), Jean-Christophe CORVOL (France), Augusto Claudio CUELLO (Canada), Jeffrey L.

CUMMINGS (USA), Herman DEPYPERE (Belgium), Bruno DUBOIS (France), Andrea DUGGENTO (Italy), Enzo EMANUELE (Italy), Valentina ESCOTT-PRICE (UK), Howard FEDEROFF (USA), Maria Teresa FERRETTI (Switzerland), Massimo FIANDACA (USA), Richard A. FRANK (USA), Francesco GARACI (Italy), Hugo GEERTS (USA), Ezio GIACOBINI (Switzerland), Filippo S. GIORGI (Italy), Edward J. GOETZL (USA), Manuela GRAZIANI (Italy), Marion HABERKAMP (Germany), Marie-Odile HABERT (France), Britta HÄNISCH (Germany), Harald HAMPEL (USA), Karl HERHOLZ (UK), Felix HERNANDEZ (Spain), Bruno P. IMBIMBO (Italy), Dimitrios KAPOGIANNIS (USA), Eric KARRAN (USA), Steven J. KIDDLE (UK), Seung H. KIM (South Korea), Yosef KORONYO (USA), Maya KORONYO-HAMAOU (USA), Todd LANGEVIN (USA), Stéphane LEHÉRICY (France), Pablo LEMERCIER (France), Simone LISTA (France), Francisco LLAVERO (Spain), Jean LORENCEAU (France), Alejandro LUCÍA (Spain), Dalila MANGO (Italy), Mark MAPSTONE (USA), Christian NERI (France), Robert NISTICÒ (Italy), Sid E. O'BRYANT (USA), Giovanni PALERMO (Italy), George PERRY (USA), Craig RITCHIE (Scotland), Simone ROSSI (Italy), Amira SAIDI (Italy), Emiliano SANTARNECCHI (USA), Lon S. SCHNEIDER (USA), Olaf SPORNS (USA), Nicola TOSCHI (Italy), Pedro L. VALENZUELA (Spain), Bruno VELLAS (France) Steven R. VERDOONER (USA), Andrea VERGALLO (USA), Nicolas VILLAIN (USA), Kelly VIRECOULON GIUDICI (France), Mark WATLING (UK), Lindsay A. WELIKOVITCH (Canada), Janet WOODCOCK (USA), Erfan YOUNESI (France), José L. ZUGAZA (Spain).

Competing interests

AV is an employee of Eisai Inc. Before November 2019 he had he received lecture honoraria from Roche, MagQu LLC, and Servier.

SL received lecture honoraria from Roche and Servier.

HZ and **KB** are co-founders of Brain Biomarker Solutions in Gothenburg AB, a GU Ventures-based platform company at the University of Gothenburg. **HZ** has served at scientific advisory boards for Roche Diagnostics, CogRx, Samumed and Wave, and has given lectures in symposia sponsored by Alzecure and Biogen. **KB** has served as a consultant or at advisory boards for Alzheon, CogRx, Biogen, Lilly, Novartis and Roche Diagnostics.

MOH has received consultant's honoraria from GE Healthcare, AVID-LILLY and PIRAMAL.

BD reports personal fees from Eli Lilly and company.

HH is an employee of Eisai Inc. and serves as Senior Associate Editor for the Journal Alzheimer's & Dementia and does not receive any fees or honoraria since May 2019; before May 2019 he had received lecture fees from Servier, Biogen and Roche, research grants from Pfizer, Avid, and MSD Avenir (paid to the institution), travel funding from Functional Neuromodulation, Axovant, Eli Lilly and company, Takeda and Zinfandel, GE-Healthcare and Oryzon Genomics, consultancy fees from Qynapse, Jung Diagnostics, Cytox Ltd., Axovant, Anavex, Takeda and Zinfandel, GE Healthcare and Oryzon Genomics, and Functional Neuromodulation, and participated in scientific advisory boards of Functional Neuromodulation, Axovant, Eisai, Eli Lilly and company, Cytox Ltd., GE Healthcare, Takeda and Zinfandel, Oryzon Genomics and Roche Diagnostics.

He is co-inventor in the following patents as a scientific expert and has received no royalties:

- *In Vitro* Multiparameter Determination Method for The Diagnosis and Early Diagnosis of Neurodegenerative Disorders Patent Number: 8916388

- *In Vitro* Procedure for Diagnosis and Early Diagnosis of Neurodegenerative Diseases Patent Number: 8298784

- Neurodegenerative Markers for Psychiatric Conditions Publication Number: 20120196300
- *In Vitro* Multiparameter Determination Method for The Diagnosis and Early Diagnosis of Neurodegenerative Disorders Publication Number: 20100062463
- *In Vitro* Method for The Diagnosis and Early Diagnosis of Neurodegenerative Disorders Publication Number: 20100035286
- *In Vitro* Procedure for Diagnosis and Early Diagnosis of Neurodegenerative Diseases Publication Number: 20090263822
- *In Vitro* Method for The Diagnosis of Neurodegenerative Diseases Patent Number: 7547553
- CSF Diagnostic in Vitro Method for Diagnosis of Dementias and Neuroinflammatory Diseases Publication Number: 20080206797
- *In Vitro* Method for The Diagnosis of Neurodegenerative Diseases Publication Number: 20080199966
- Neurodegenerative Markers for Psychiatric Conditions Publication Number: 20080131921

PL, PAC, MCP, FB, EC, and FC report no competing interests.

References

- Acaz-Fonseca, E., Duran, J.C., Carrero, P., Garcia-Segura, L.M., Arevalo, M.A., 2015. Sex differences in glia reactivity after cortical brain injury. *Glia* 63, 1966–1981. <https://doi.org/10.1002/glia.22867>
- Alcolea, D., Carmona-Iragui, M., Suarez-Calvet, M., Sanchez-Saudinos, M.B., Sala, I., Anton-Aguirre, S., Blesa, R., Clarimon, J., Fortea, J., Lleo, A., 2014. Relationship between beta-Secretase, inflammation and core cerebrospinal fluid biomarkers for Alzheimer's disease. *J. Alzheimers. Dis.* 42, 157–167. <https://doi.org/10.3233/JAD-140240>
- Alcolea, D., Martinez-Lage, P., Sanchez-Juan, P., Olazaran, J., Antunez, C., Izagirre, A., Ecay-Torres, M., Estanga, A., Clerigue, M., Guisasola, M.C., Sanchez Ruiz, D., Marin Munoz, J., Calero, M., Blesa, R., Clarimon, J., Carmona-Iragui, M., Morenas-Rodriguez, E., Rodriguez-Rodriguez, E., Vazquez Higuera, J.L., Fortea, J., Lleo, A., 2015. Amyloid precursor protein metabolism and inflammation markers in preclinical Alzheimer disease. *Neurology* 85, 626–633. <https://doi.org/10.1212/WNL.0000000000001859>
- Antonell, A., Mansilla, A., Rami, L., Llado, A., Iranzo, A., Olives, J., Balasa, M., Sanchez-Valle, R., Molinuevo, J.L., 2014. Cerebrospinal fluid level of YKL-40 protein in preclinical and prodromal Alzheimer's disease. *J. Alzheimers. Dis.* 42, 901–908. <https://doi.org/10.3233/JAD-140624>
- Arranz, A.M., De Strooper, B., 2019. The role of astroglia in Alzheimer's disease: pathophysiology and clinical implications. *Lancet. Neurol.* 18, 406–414. [https://doi.org/10.1016/S1474-4422\(18\)30490-3](https://doi.org/10.1016/S1474-4422(18)30490-3)
- Baldacci, F., Lista, S., Cavedo, E., Bonuccelli, U., Hampel, H., 2017. Diagnostic function of the neuroinflammatory biomarker YKL-40 in Alzheimer's disease and other neurodegenerative diseases. *Expert Rev. Proteomics* 14, 285–299. <https://doi.org/10.1080/14789450.2017.1304217>
- Baldacci, F., Lista, S., Palermo, G., Giorgi, F.S., Vergallo, A., Hampel, H., 2019. The neuroinflammatory biomarker YKL-40 for neurodegenerative diseases: advances in development. *Expert Rev. Proteomics* 16, 593–600. <https://doi.org/10.1080/14789450.2019.1628643>
- Bonneh-Barkay, D., Bissel, S.J., Kofler, J., Starkey, A., Wang, G., Wiley, C.A., 2012. Astrocyte and macrophage regulation of YKL-40 expression and cellular response in neuroinflammation. *Brain Pathol.* 22, 530–546. <https://doi.org/10.1111/j.1750-3639.2011.00550.x>
- Buckley, R.F., Maruff, P., Ames, D., Bourgeat, P., Martins, R.N., Masters, C.L., Rainey-Smith, S., Lautenschlager, N., Rowe, C.C., Savage, G., Villemagne, V.L., Ellis, K.A., 2016. Subjective memory decline predicts greater rates of clinical progression in preclinical Alzheimer's disease. *Alzheimers. Dement.* 12, 796–804. <https://doi.org/10.1016/j.jalz.2015.12.013>
- Cavedo, E., Chiesa, P.A., Houot, M., Ferretti, M.T., Grothe, M.J., Teipel, S.J., Lista, S., Habert, M.-O., Potier, M.-C., Dubois, B., Hampel, H., 2018. Sex differences in functional and molecular neuroimaging biomarkers of Alzheimer's disease in cognitively normal older adults with subjective memory complaints. *Alzheimers. Dement.* 14, 1204–1215. <https://doi.org/10.1016/j.jalz.2018.05.014>
- Choi, J., Lee, H.-W., Suk, K., 2011. Plasma level of chitinase 3-like 1 protein increases in patients with early Alzheimer's disease. *J. Neurol.* 258, 2181–2185. <https://doi.org/10.1007/s00415-011-6087-9>
- Craig-Schapiro, R., Perrin, R.J., Roe, C.M., Xiong, C., Carter, D., Cairns, N.J., Mintun, M.A., Peskind, E.R., Li, G., Galasko, D.R., Clark, C.M., Quinn, J.F., D'Angelo, G., Malone,

- J.P., Townsend, R.R., Morris, J.C., Fagan, A.M., Holtzman, D.M., 2010. YKL-40: a novel prognostic fluid biomarker for preclinical Alzheimer's disease. *Biol. Psychiatry* 68, 903–912. <https://doi.org/10.1016/j.biopsych.2010.08.025>
- De Strooper, B., Karran, E., 2016. The Cellular Phase of Alzheimer's Disease. *Cell* 164, 603–615. <https://doi.org/10.1016/j.cell.2015.12.056>
- Dubois, B., Epelbaum, S., Nyasse, F., Bakardjian, H., Gagliardi, G., Uspenskaya, O., Houot, M., Lista, S., Cacciamani, F., Potier, M.-C., Bertrand, A., Lamari, F., Benali, H., Mangin, J.-F., Colliot, O., Genthon, R., Habert, M.-O., Hampel, H., 2018. Cognitive and neuroimaging features and brain beta-amyloidosis in individuals at risk of Alzheimer's disease (INSIGHT-preAD): a longitudinal observational study. *Lancet. Neurol.* 17, 335–346. [https://doi.org/10.1016/S1474-4422\(18\)30029-2](https://doi.org/10.1016/S1474-4422(18)30029-2)
- Edwards, F.A., 2019. A Unifying Hypothesis for Alzheimer's Disease: From Plaques to Neurodegeneration. *Trends Neurosci.* 42, 310–322. <https://doi.org/10.1016/j.tins.2019.03.003>
- Edwards, L.J., 2000. Modern statistical techniques for the analysis of longitudinal data in biomedical research. *Pediatr. Pulmonol.* 30, 330–344.
- Falcon, C., Monte-Rubio, G.C., Grau-Rivera, O., Suarez-Calvet, M., Sanchez-Valle, R., Rami, L., Bosch, B., Haass, C., Gispert, J.D., Molinuevo, J.L., 2019. CSF glial biomarkers YKL40 and sTREM2 are associated with longitudinal volume and diffusivity changes in cognitively unimpaired individuals. *NeuroImage. Clin.* 23, 101801. <https://doi.org/10.1016/j.nicl.2019.101801>
- Gagliardi, G., Epelbaum, S., Houot, M., Bakardjian, H., Boukadida, L., Revillon, M., Dubois, B., Dalla Barba, G., La Corte, V., & INSIGHT-preAD study group, 2019. Which Episodic Memory Performance is Associated with Alzheimer's Disease Biomarkers in Elderly Cognitive Complainers? Evidence from a Longitudinal Observational Study with Four Episodic Memory Tests (Insight-PreAD). *J Alzheimers Dis.* 70, 811-824. <https://doi:10.3233/JAD-180966>
- Gispert, J.D., Monte, G.C., Falcon, C., Tucholka, A., Rojas, S., Sanchez-Valle, R., Antonell, A., Llado, A., Rami, L., Molinuevo, J.L., 2016. CSF YKL-40 and pTau181 are related to different cerebral morphometric patterns in early AD. *Neurobiol. Aging* 38, 47–55. <https://doi.org/10.1016/j.neurobiolaging.2015.10.022>
- Gomez-Arboledas, A., Davila, J.C., Sanchez-Mejias, E., Navarro, V., Nunez-Diaz, C., Sanchez-Varo, R., Sanchez-Mico, M.V., Trujillo-Estrada, L., Fernandez-Valenzuela, J.J., Vizuete, M., Comella, J.X., Galea, E., Vitorica, J., Gutierrez, A., 2018. Phagocytic clearance of presynaptic dystrophies by reactive astrocytes in Alzheimer's disease. *Glia* 66, 637–653. <https://doi.org/10.1002/glia.23270>
- Graham, L.C., Naldrett, M.J., Kohama, S.G., Smith, C., Lamont, D.J., McColl, B.W., Gillingwater, T.H., Skehel, P., Urbanski, H.F., Wishart, T.M., 2019. Regional Molecular Mapping of Primate Synapses during Normal Healthy Aging. *Cell Rep.* 27, 1018----1026.e4. <https://doi.org/10.1016/j.celrep.2019.03.096>
- Grewal, R., Haghighi, M., Huang, S., Smith, A.G., Cao, C., Lin, X., Lee, D.C., Teten, N., Hill, A.M., Selenica, M.-L.B., 2016. Identifying biomarkers of dementia prevalent among amnesic mild cognitively impaired ethnic female patients. *Alzheimers. Res. Ther.* 8, 43. <https://doi.org/10.1186/s13195-016-0211-0>
- Guan, R., Lin, R., Jin, R., Lu, L., Liu, X., Hu, S., Sun, L., 2019. Chitinase-like protein YKL-40 regulates human bronchial epithelial cells proliferation, apoptosis, and migration through TGF-beta1/Smads pathway. *Hum. Exp. Toxicol.* 960327119891218. <https://doi.org/10.1177/0960327119891218>
- Guerra-Gomes, S., Sousa, N., Pinto, L., Oliveira, J.F., 2017. Functional Roles of Astrocyte Calcium Elevations: From Synapses to Behavior. *Front. Cell. Neurosci.* 11, 427.

<https://doi.org/10.3389/fncel.2017.00427>

- Habert, M.-O., Bertin, H., Labit, M., Diallo, M., Marie, S., Martineau, K., Kas, A., Causse-Lemercier, V., Bakardjian, H., Epelbaum, S., Chetelat, G., Houot, M., Hampel, H., Dubois, B., Mangin, J.-F., 2018. Evaluation of amyloid status in a cohort of elderly individuals with memory complaints: validation of the method of quantification and determination of positivity thresholds. *Ann. Nucl. Med.* 32, 75–86.
<https://doi.org/10.1007/s12149-017-1221-0>
- Hampel, H., Lista, S., Neri, C., Vergallo, A., 2019a. Time for the systems-level integration of aging: Resilience enhancing strategies to prevent Alzheimer's disease. *Prog. Neurobiol.* 101662. <https://doi.org/10.1016/j.pneurobio.2019.101662>
- Hampel, H., O'Bryant, S.E., Molinuevo, J.L., Zetterberg, H., Masters, C.L., Lista, S., Kiddle, S.J., Batrla, R., Blennow, K., 2018a. Blood-based biomarkers for Alzheimer disease: mapping the road to the clinic. *Nat. Rev. Neurol.* 14, 639–652.
<https://doi.org/10.1038/s41582-018-0079-7>
- Hampel, H., Toschi, N., Babiloni, C., Baldacci, F., Black, K.L., Bokde, A.L.W., Bun, R.S., Cacciola, F., Cavedo, E., Chiesa, P.A., Colliot, O., Coman, C.-M., Dubois, B., Duggento, A., Durrleman, S., Ferretti, M.-T., George, N., Genthon, R., Habert, M.-O., Herholz, K., Koronyo, Y., Koronyo-Hamaoui, M., Lamari, F., Langevin, T., Lehericy, S., Lorenceau, J., Neri, C., Nistico, R., Nyasse-Messene, F., Ritchie, C., Rossi, S., Santarnecchi, E., Sporns, O., Verdooner, S.R., Vergallo, A., Villain, N., Younesi, E., Garaci, F., Lista, S., 2018b. Revolution of Alzheimer Precision Neurology. *Passageway of Systems Biology and Neurophysiology. J. Alzheimers. Dis.* 64, S47--S105. <https://doi.org/10.3233/JAD-179932>
- Hampel, H., Vergallo, A., Perry, G., Lista, S., 2019b. The Alzheimer Precision Medicine Initiative. *J. Alzheimers. Dis.* 68, 1–24. <https://doi.org/10.3233/JAD-181121>
- Hellwig, K., Kvartsberg, H., Portelius, E., Andreasson, U., Oberstein, T.J., Lewczuk, P., Blennow, K., Kornhuber, J., Maler, J.M., Zetterberg, H., Spitzer, P., 2015. Neurogranin and YKL-40: independent markers of synaptic degeneration and neuroinflammation in Alzheimer's disease. *Alzheimers. Res. Ther.* 7, 74. <https://doi.org/10.1186/s13195-015-0161-y>
- Hellwig, S., Masuch, A., Nestel, S., Katzmarski, N., Meyer-Luehmann, M., Biber, K., 2015. Forebrain microglia from wild-type but not adult 5xFAD mice prevent amyloid-beta plaque formation in organotypic hippocampal slice cultures. *Sci. Rep.* 5, 14624.
<https://doi.org/10.1038/srep14624>
- Heneka, M.T., Carson, M.J., El Khoury, J., Landreth, G.E., Brosseron, F., Feinstein, D.L., Jacobs, A.H., Wyss-Coray, T., Vitorica, J., Ransohoff, R.M., Herrup, K., Frautschy, S.A., Finsen, B., Brown, G.C., Verkhratsky, A., Yamanaka, K., Koistinaho, J., Latz, E., Halle, A., Petzold, G.C., Town, T., Morgan, D., Shinohara, M.L., Perry, V.H., Holmes, C., Bazan, N.G., Brooks, D.J., Hunot, S., Joseph, B., Deigendesch, N., Garaschuk, O., Boddeke, E., Dinarello, C.A., Breitner, J.C., Cole, G.M., Golenbock, D.T., Kummer, M.P., 2015. Neuroinflammation in Alzheimer's disease. *Lancet. Neurol.* 14, 388–405.
[https://doi.org/10.1016/S1474-4422\(15\)70016-5](https://doi.org/10.1016/S1474-4422(15)70016-5)
- Heppner, F.L., Ransohoff, R.M., Becher, B., 2015. Immune attack: the role of inflammation in Alzheimer disease. *Nat. Rev. Neurosci.* 16, 358–372. <https://doi.org/10.1038/nrn3880>
- Janelidze, S., Mattsson, N., Stomrud, E., Lindberg, O., Palmqvist, S., Zetterberg, H., Blennow, K., Hansson, O., 2018. CSF biomarkers of neuroinflammation and cerebrovascular dysfunction in early Alzheimer disease. *Neurology* 91, e867----e877.
<https://doi.org/10.1212/WNL.0000000000006082>
- Kester, M.I., Teunissen, C.E., Sutphen, C., Herries, E.M., Ladenson, J.H., Xiong, C., Scheltens, P., van der Flier, W.M., Morris, J.C., Holtzman, D.M., Fagan, A.M., 2015.

- Cerebrospinal fluid VILIP-1 and YKL-40, candidate biomarkers to diagnose, predict and monitor Alzheimer's disease in a memory clinic cohort. *Alzheimers. Res. Ther.* 7, 59. <https://doi.org/10.1186/s13195-015-0142-1>
- Kim, J., Jiang, H., Park, S., Eltorai, A.E.M., Stewart, F.R., Yoon, H., Basak, J.M., Finn, M.B., Holtzman, D.M., 2011. Haploinsufficiency of human APOE reduces amyloid deposition in a mouse model of amyloid-beta amyloidosis. *J. Neurosci.* 31, 18007–18012. <https://doi.org/10.1523/JNEUROSCI.3773-11.2011>
- Krasemann, S., Madore, C., Cialic, R., Baufeld, C., Calcagno, N., El Fatimy, R., Beckers, L., O'Loughlin, E., Xu, Y., Fanek, Z., Greco, D.J., Smith, S.T., Tweet, G., Humulock, Z., Zrzavy, T., Conde-Sanroman, P., Gacias, M., Weng, Z., Chen, H., Tjon, E., Mazaheri, F., Hartmann, K., Madi, A., Ulrich, J.D., Glatzel, M., Worthmann, A., Heeren, J., Budnik, B., Lemere, C., Ikezu, T., Heppner, F.L., Litvak, V., Holtzman, D.M., Lassmann, H., Weiner, H.L., Ochando, J., Haass, C., Butovsky, O., 2017. The TREM2-APOE Pathway Drives the Transcriptional Phenotype of Dysfunctional Microglia in Neurodegenerative Diseases. *Immunity* 47, 566–581.e9. <https://doi.org/10.1016/j.immuni.2017.08.008>
- Lleo, A., Alcolea, D., Martinez-Lage, P., Scheltens, P., Parnetti, L., Poirier, J., Simonsen, A.H., Verbeek, M.M., Rosa-Neto, P., Slot, R.E.R., Tainta, M., Izaguirre, A., Reijls, B.L.R., Farotti, L., Tsolaki, M., Vandenbergue, R., Freund-Levi, Y., Verhey, F.R.J., Clarimon, J., Fortea, J., Frolich, L., Santana, I., Molinuevo, J.L., Lehmann, S., Visser, P.J., Teunissen, C.E., Zetterberg, H., Blennow, K., 2019. Longitudinal cerebrospinal fluid biomarker trajectories along the Alzheimer's disease continuum in the BIOMARKAPD study. *Alzheimers. Dement.* 15, 742–753. <https://doi.org/10.1016/j.jalz.2019.01.015>
- Luke, S.G., 2017. Evaluating significance in linear mixed-effects models in R. *Behav. Res. Methods* 49, 1494–1502. <https://doi.org/10.3758/s13428-016-0809-y>
- McCarthy, M.M., Nugent, B.M., Lenz, K.M., 2017. Neuroimmunology and neuroepigenetics in the establishment of sex differences in the brain. *Nat. Rev. Neurosci.* 18, 471–484. <https://doi.org/10.1038/nrn.2017.61>
- Molinuevo, J.L., Ayton, S., Batrla, R., Bednar, M.M., Bittner, T., Cummings, J., Fagan, A.M., Hampel, H., Mielke, M.M., Mikulskis, A., O'Bryant, S., Scheltens, P., Sevigny, J., Shaw, L.M., Soares, H.D., Tong, G., Trojanowski, J.Q., Zetterberg, H., Blennow, K., 2018. Current state of Alzheimer's fluid biomarkers. *Acta Neuropathol.* 136, 821–853. <https://doi.org/10.1007/s00401-018-1932-x>
- Oide, T., Kinoshita, T., Arima, K., 2006. Regression stage senile plaques in the natural course of Alzheimer's disease. *Neuropathol. Appl. Neurobiol.* 32, 539–556. <https://doi.org/10.1111/j.1365-2990.2006.00767.x>
- Olsson, B., Lautner, R., Andreasson, U., Ohrfelt, A., Portelius, E., Bjerke, M., Holtta, M., Rosen, C., Olsson, C., Strobel, G., Wu, E., Dakin, K., Petzold, M., Blennow, K., Zetterberg, H., 2016. CSF and blood biomarkers for the diagnosis of Alzheimer's disease: a systematic review and meta-analysis. *Lancet. Neurol.* 15, 673–684. [https://doi.org/10.1016/S1474-4422\(16\)00070-3](https://doi.org/10.1016/S1474-4422(16)00070-3)
- Perez-Nievas, B.G., Serrano-Pozo, A., 2018. Deciphering the Astrocyte Reaction in Alzheimer's Disease. *Front. Aging Neurosci.* 10, 114. <https://doi.org/10.3389/fnagi.2018.00114>
- Pierscianek, D., Ahmadipour, Y., Oppong, M.D., Rauschenbach, L., Kebir, S., Glas, M., Sure, U., Jabbarli, R., 2019. Blood-Based Biomarkers in High Grade Gliomas: a Systematic Review. *Mol. Neurobiol.* <https://doi.org/10.1007/s12035-019-1509-2>
- Pihlaja, R., Koistinaho, J., Malm, T., Sikkila, H., Vainio, S., Koistinaho, M., 2008. Transplanted astrocytes internalize deposited beta-amyloid peptides in a transgenic mouse model of Alzheimer's disease. *Glia* 56, 154–163.

<https://doi.org/10.1002/glia.20599>

- Rawji, K.S., Mishra, M.K., Michaels, N.J., Rivest, S., Stys, P.K., Yong, V.W., 2016. Immunosenescence of microglia and macrophages: impact on the ageing central nervous system. *Brain* 139, 653–661. <https://doi.org/10.1093/brain/awv395>
- Santos-Galindo, M., Acaz-Fonseca, E., Bellini, M.J., Garcia-Segura, L.M., 2011. Sex differences in the inflammatory response of primary astrocytes to lipopolysaccharide. *Biol. Sex Differ.* 2, 7. <https://doi.org/10.1186/2042-6410-2-7>
- SATTERTHWAITE, F.E., 1946. An approximate distribution of estimates of variance components. *Biometrics* 2, 110–114.
- Schwarz, J.M., McCarthy, M.M., 2008. Steroid-induced sexual differentiation of the developing brain: multiple pathways, one goal. *J. Neurochem.* 105, 1561–1572. <https://doi.org/10.1111/j.1471-4159.2008.05384.x>
- Serrano-Pozo, A., Muzikansky, A., Gomez-Isla, T., Growdon, J.H., Betensky, R.A., Frosch, M.P., Hyman, B.T., 2013. Differential relationships of reactive astrocytes and microglia to fibrillar amyloid deposits in Alzheimer disease. *J. Neuropathol. Exp. Neurol.* 72, 462–471. <https://doi.org/10.1097/NEN.0b013e3182933788>
- Shi, Y., Holtzman, D.M., 2018. Interplay between innate immunity and Alzheimer disease: APOE and TREM2 in the spotlight. *Nat. Rev. Immunol.* 18, 759–772. <https://doi.org/10.1038/s41577-018-0051-1>
- Shi, Y., Yamada, K., Liddelov, S.A., Smith, S.T., Zhao, L., Luo, W., Tsai, R.M., Spina, S., Grinberg, L.T., Rojas, J.C., Gallardo, G., Wang, K., Roh, J., Robinson, G., Finn, M.B., Jiang, H., Sullivan, P.M., Baufeld, C., Wood, M.W., Sutphen, C., McCue, L., Xiong, C., Del-Aguila, J.L., Morris, J.C., Cruchaga, C., Fagan, A.M., Miller, B.L., Boxer, A.L., Seeley, W.W., Butovsky, O., Barres, B.A., Paul, S.M., Holtzman, D.M., 2017. ApoE4 markedly exacerbates tau-mediated neurodegeneration in a mouse model of tauopathy. *Nature* 549, 523–527. <https://doi.org/10.1038/nature24016>
- Shin, S., Walz, K.A., Archambault, A.S., Sim, J., Bollman, B.P., Koenigsnecht-Talboo, J., Cross, A.H., Holtzman, D.M., Wu, G.F., 2014. Apolipoprotein E mediation of neuroinflammation in a murine model of multiple sclerosis. *J. Neuroimmunol.* 271, 8–17. <https://doi.org/10.1016/j.jneuroim.2014.03.010>
- Streit, W.J., Braak, H., Xue, Q.-S., Bechmann, I., 2009. Dystrophic (senescent) rather than activated microglial cells are associated with tau pathology and likely precede neurodegeneration in Alzheimer's disease. *Acta Neuropathol.* 118, 475–485. <https://doi.org/10.1007/s00401-009-0556-6>
- Twisk, J., de Boer, M., de Vente, W., Heymans, M., 2013. Multiple imputation of missing values was not necessary before performing a longitudinal mixed-model analysis. *J. Clin. Epidemiol.* 66, 1022–1028. <https://doi.org/10.1016/j.jclinepi.2013.03.017>
- van Harten, A.C., Mielke, M.M., Swenson-Dravis, D.M., Hagen, C.E., Edwards, K.K., Roberts, R.O., Geda, Y.E., Knopman, D.S., Petersen, R.C., 2018. Subjective cognitive decline and risk of MCI: The Mayo Clinic Study of Aging. *Neurology* 91, e300---e312. <https://doi.org/10.1212/WNL.0000000000005863>
- VanRyzin, J.W., Pickett, L.A., McCarthy, M.M., 2018. Microglia: Driving critical periods and sexual differentiation of the brain. *Dev. Neurobiol.* 78, 580–592. <https://doi.org/10.1002/dneu.22569>
- Vergallo, A., Megret, L., Lista, S., Cavedo, E., Zetterberg, H., Blennow, K., Vanmechelen, E., De Vos, A., Habert, M.-O., Potier, M.-C., Dubois, B., Neri, C., Hampel, H., 2019. Plasma amyloid beta 40/42 ratio predicts cerebral amyloidosis in cognitively normal individuals at risk for Alzheimer's disease. *Alzheimers. Dement.* 15, 764–775. <https://doi.org/10.1016/j.jalz.2019.03.009>
- Vest, R.S., Pike, C.J., 2013. Gender, sex steroid hormones, and Alzheimer's disease. *Horm.*

- Behav. 63, 301–307. <https://doi.org/10.1016/j.yhbeh.2012.04.006>
- Villa, A., Gelosa, P., Castiglioni, L., Cimino, M., Rizzi, N., Pepe, G., Lolli, F., Marcello, E., Sironi, L., Vegeto, E., Maggi, A., 2018. Sex-Specific Features of Microglia from Adult Mice. *Cell Rep.* 23, 3501–3511. <https://doi.org/10.1016/j.celrep.2018.05.048>
- Wolf, D., Bocchetta, M., Preboske, G.M., Boccardi, M., Grothe, M.J., 2017. Reference standard space hippocampus labels according to the European Alzheimer’s Disease Consortium-Alzheimer’s Disease Neuroimaging Initiative harmonized protocol: Utility in automated volumetry. *Alzheimers. Dement.* 13, 893–902. <https://doi.org/10.1016/j.jalz.2017.01.009>
- Wyss-Coray, T., Loike, J.D., Brionne, T.C., Lu, E., Anankov, R., Yan, F., Silverstein, S.C., Husemann, J., 2003. Adult mouse astrocytes degrade amyloid-beta in vitro and in situ. *Nat. Med.* 9, 453–457. <https://doi.org/10.1038/nm838>
- Zhang, H., Tan, J.-Z., Luo, J., Wang, W., 2019. Chitinase-3-like protein 1 may be a potential biomarker in patients with drug-resistant epilepsy. *Neurochem. Int.* 124, 62–67. <https://doi.org/10.1016/j.neuint.2018.12.013>
- Zhang, L., shing Li, B., Zhao, W., Chang, Y.H., Ma, W., Dragan, M., Barker, J.L., Hu, Q., Rubinow, D.R., 2002. Sex-related differences in MAPKs activation in rat astrocytes: effects of estrogen on cell death. *Brain Res. Mol. Brain Res.* 103, 1–11.
- Zhao, R., Hu, W., Tsai, J., Li, W., Gan, W.-B., 2017. Microglia limit the expansion of beta-amyloid plaques in a mouse model of Alzheimer’s disease. *Mol. Neurodegener.* 12, 47. <https://doi.org/10.1186/s13024-017-0188-6>

FIGURE LEGENDS

Figure 1. Difference in plasma YKL-40 concentrations between sexes.

Note: The figure shows higher YKL-40 concentrations in men compared to women, at baseline ($b=0.151$, Cohen's $f^2=0.014$, $P=0.036$, adjusted $P=0.054$).

Plasma YKL-40 concentrations are expressed in terms of the logarithm of pg/mL.

The significant difference between sexes was found at each time point and, here, we show the difference at baseline.

Abbreviations: F = female; Log = logarithmic transformation; M = male; P = p-value.

Figure 2. Difference in longitudinal trajectories of plasma YKL-40 concentrations across sexes.

Note: The figure shows higher YKL-40 concentrations in men compared to women at all time-points investigated ($b=0.171$, Cohen's $f^2=0.017$, $P=0.015$, adjusted $P=0.023$). No significant two-way interaction of time and sex on YKL-40 was found.

Plasma YKL-40 concentrations are expressed in terms of the logarithm of pg/mL.

Abbreviations: Log = logarithmic transformation; M0 = baseline; M12 = one-year follow-up; M36 = three-year follow-up; P = p-value.

Figure 3. Association between longitudinal trajectories of plasma YKL-40 concentrations and age at baseline.

Note: The figure shows a positive association between plasma YKL-40 concentrations and age at baseline ($b=0.028$, Cohen's $f^2=0.027$, $P=0.004$, adjusted $P=0.012$). Such a significant association is present at each time-point. No significant effect of the interaction between time and age was found.

Plasma YKL-40 concentrations are expressed in terms of the logarithm of pg/mL. Grey bands represent 95% confidence interval.

Abbreviations: Log = logarithmic transformation; M0 = baseline; M12 = one-year follow-up; M36 = three-year follow-up; P = p-value.

Figure 4. Association between plasma YKL-40 concentration and global A β -PET SUVR at baseline.

Note: The figure shows a negative correlation between plasma YKL-40 concentrations and baseline global A β -PET SUVR ($b=-0.025$, Cohen's $f^2=0.015$, $P=0.036$).

Plasma YKL-40 concentrations are expressed in terms of the logarithm of pg/mL. Grey bands represent 95% confidence interval. Predicted values of global A β -PET SUVR are calculated using the estimated marginal means to adjust on age, sex, and APOE $\epsilon 4$ allele.

Abbreviations: A β = amyloid beta; APOE $\epsilon 4$ = Apolipoprotein E $\epsilon 4$ allele; Log = logarithmic transformation; P = p-value; SUVR = standardized uptake value ratio.

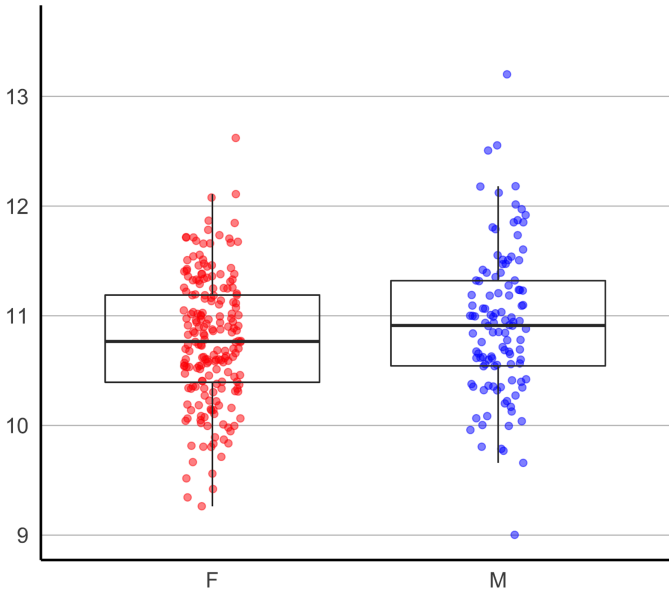
Figure 5. Association between plasma YKL-40 concentration and FCSRT total recall task.

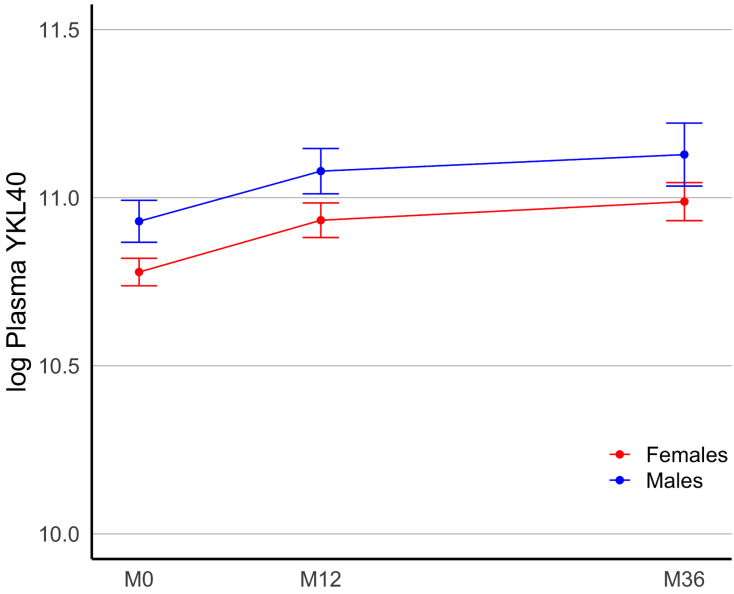
Note: The figure shows an increase of YKL-40 concentration over 1 year was positively associated with a higher FCSRT total recall score at M24 (b=0.308, Cohen's $f^2=0.005$ $P=0.023$).

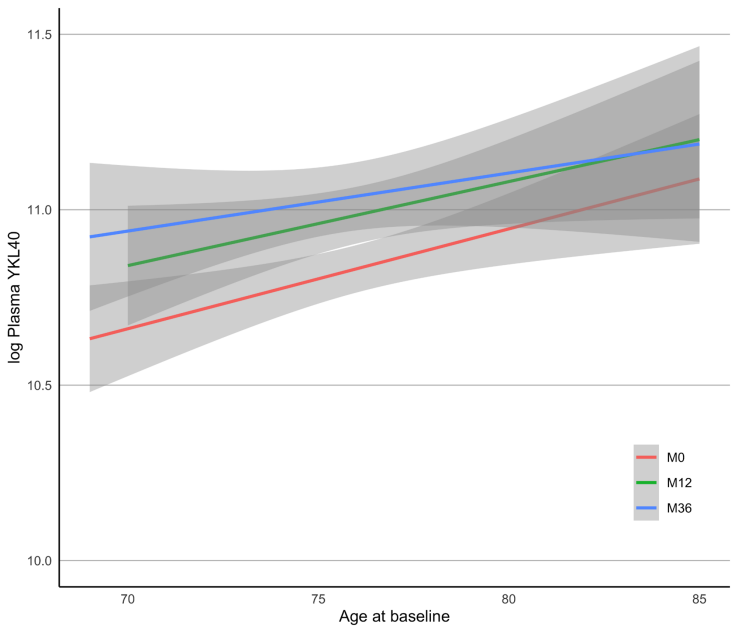
Plasma YKL-40 concentrations are expressed in terms of difference of logarithm of pg/mL between M12 and M0. Grey bands represent 95% confidence interval. Predicted **percentage score** in the FCSRT total recall task at M24 are calculated using the estimated marginal means to adjust on age, sex, and *APOE* $\epsilon 4$ allele.

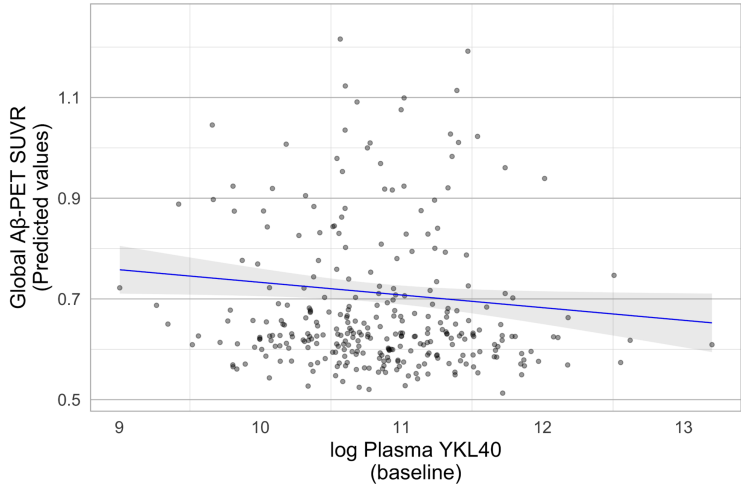
Abbreviations: *APOE* $\epsilon 4$ = Apolipoprotein E $\epsilon 4$ allele; FCSRT = Free and Cued Selective Reminding Test; Log = logarithmic transformation; M0 = baseline; M12 = one-year follow-up; M24 = two-year follow-up; P = p-value.

log Plasma YKL40
(baseline)









FCSRT total recall
(Predicted score at M24)

100%
95%
90%
85%

-0.5

log Plasma YKL40
(M12-M0)

0.5

1.0

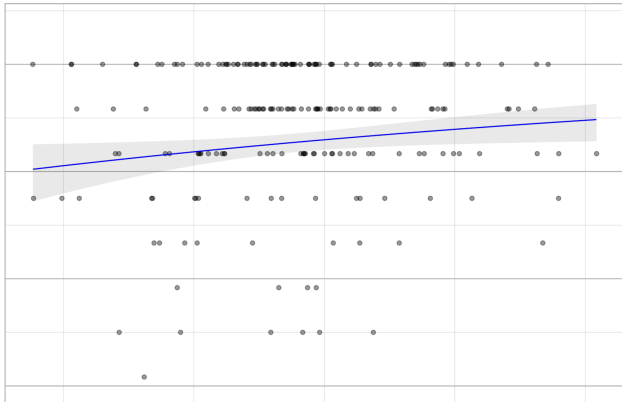


Table 1. Cohort description at baseline and over the time.

	M0 N=314	M12 N=227	M36 N=131
Plasma log YKL-40 concentration (pg/mL), mean \pm SD	10.83 \pm 0.62	10.99 \pm 0.62	11.03 \pm 0.56
Sex, n of females	200	137	89
Age at baseline, mean \pm SD	76.07 \pm 3.51	76.07 \pm 3.51	76.07 \pm 3.51
APOE ϵ4 allele carriers, n	252	181	101

Abbreviations: APOE ϵ 4= Apolipoprotein E ϵ 4 allele; M0= baseline; M12= one-year follow-up; M36= three-year follow-up; n= number of participants; SD= standard deviation.

Table 2. Associations between main biological factors and plasma YKL-40 concentrations at baseline and over the time.

	Baseline*				Follow-up**							
	Coefficient [95% CI]	t-value	P-value (adjusted)	Cohen's f ²	Main effect				Time interaction			
Coefficient [95% CI]					t-value	P-value (adjusted)	Cohen's f ²	Coefficient [95% CI]	t-value	P-value (adjusted)	Cohen's f ²	
Sex	0.151 [0.010; 0.292]	2.101	0.036 (0.054)	0.014	0.171 [0.033; 0.308]	2.434	0.015 (0.023)	0.017	0.002 [-0.048; 0.052]	0.077	0.939 (0.939)	1.55e ⁻⁵
Age at baseline	0.028 [0.009; 0.048]	2.909	0.004 (0.012)	0.027	0.029 [0.010; 0.048]	3.044	0.003 (0.009)	0.027	3.95e ⁻⁴ [-0.006; 0.007]	0.113	0.910 (0.939)	4.47e ⁻⁵
APOE ε4 allele	-0.032 [-0.140; 0.204]	-0.368	0.713 (0.713)	4.34e ⁻⁴	-0.013 [-0.154; 0.180]	-0.148	0.883 (0.883)	1.01e ⁻⁴	0.041 [-0.098; 0.016]	1.418	0.157 (0.471)	0.001

Abbreviations: APOE ε4 = Apolipoprotein E ε4 allele.

*Linear model was used to test the effect of variable of interest on plasma YKL-40 concentration

**Linear mixed model was used to test the main effect and time interaction of variable of interest on plasma YKL-40 concentration

Table 3. Associations between baseline plasma YKL-40 concentrations and A β -PET SUVR at baseline and over the two-year follow-up.

	M0 (302)	M24 (255)	Baseline*				Follow-up**								
							Main effect				Time interaction				
			Mean \pm SD	Mean \pm SD	Coefficient [95% CI]	t-value	P-value (adjusted)	Cohen's f ²	Coefficient [95% CI]	t-value	P-value (adjusted)	Cohen's f ²	Coefficient [95% CI]	t-value	P-value (adjusted)
Global SUVR	0.677 \pm 0.134	0.696 \pm 0.136	-0.025 [-0.049; -0.002]	-2.102	0.036	0.015	-0.025 [-0.049; -0.001]	-1.992	0.047	0.014	-5.38e ⁻⁵ [-0.004; 0.003]	-0.279	0.781	9.36e ⁻⁶	
Regional SUVR															
Left posterior cingulate cortex	0.618 \pm 0.153	0.640 \pm 0.161	-0.025 [-0.052; 0.002]	-1.797	0.073 (0.087)	0.011	-0.025 [-0.052; 0.003]	-1.714	0.087 (0.104)	0.015	-0.006 [-0.013; 4.35e ⁻⁴]	-1.831	0.068 (0.480)	8.07e ⁻⁴	
Right posterior cingulate cortex	0.599 \pm 0.148	0.622 \pm 0.153	-0.025 [-0.051; 0.001]	-1.900	0.058 (0.081)	0.012	-0.026 [-0.053; 0.001]	-1.853	0.065 (0.104)	0.014	-0.003 [-0.009; 0.003]	-0.980	0.328 (0.752)	2.17e ⁻⁴	
Left anterior cingulate cortex	0.593 \pm 0.134	0.618 \pm 0.147	-0.018 [-0.042; 0.006]	-1.492	0.137 (0.137)	0.007	-0.018 [-0.043; 0.007]	-1.373	0.171 (0.171)	0.008	-0.002 [-0.007; 0.003]	-0.774	0.440 (0.752)	9.20e ⁻⁵	
Right anterior cingulate cortex	0.618 \pm 0.142	0.630 \pm 0.144	-0.022 [-0.047; 0.003]	-1.751	0.081 (0.088)	0.010	-0.022 [-0.048; 0.004]	-1.651	0.100 (0.109)	0.008	0.002 [-0.003; 0.006]	0.630	0.530 (0.752)	7.53e ⁻⁶	
Left superior orbitofrontal cortex	0.800 \pm 0.136	0.808 \pm 0.141	-0.029 [-0.053; -0.005]	-2.377	0.018 (0.075)	0.019	-0.028 [-0.053; -0.003]	-2.212	0.028 (0.104)	0.013	0.004 [-0.001; 0.009]	1.561	0.120 (0.480)	2.01e ⁻⁴	
Right superior orbitofrontal cortex	0.776 \pm 0.137	0.788 \pm 0.143	-0.028 [-0.052; -0.004]	-2.259	0.025 (0.075)	0.017	-0.027 [-0.052; -0.002]	-2.071	0.039 (0.104)	0.016	-9.36e ⁻⁴ [-0.007; 0.005]	-0.316	0.752 (0.752)	2.50e ⁻⁵	
Left inferior parietal lobe	0.692 \pm 0.137	0.720 \pm 0.144	-0.029 [-0.053; -0.005]	-2.351	0.019 (0.075)	0.019	-0.028 [-0.053; -0.003]	-2.152	0.032 (0.104)	0.015	0.001 [-0.005; 0.007]	0.409	0.683 (0.752)	-3.34e ⁻⁵	
Right inferior parietal lobe	0.689 \pm 0.146	0.707 \pm 0.141	-0.030 [-0.056; -0.004]	-2.304	0.022 (0.075)	0.018	-0.029 [-0.055; -0.004]	-2.214	0.028 (0.104)	0.016	0.001 [-0.005; 0.007]	0.371	0.711 (0.752)	-2.69e ⁻⁵	
Left precuneus	0.667 \pm 0.145	0.690 \pm 0.146	-0.025 [-0.051; 0.001]	-1.898	0.059 (0.081)	0.012	-0.025 [-0.051; 0.001]	-1.877	0.062 (0.104)	0.011	0.001 [-0.004; 0.006]	0.512	0.609 (0.752)	-3.19e ⁻⁶	
Right precuneus	0.662 \pm 0.147	0.686 \pm 0.149	-0.025 [-0.052; 0.001]	-1.926	0.055 (0.081)	0.012	-0.026 [-0.052; 0.001]	-1.864	0.063 (0.104)	0.016	-0.005 [-0.010; 0.001]	-1.745	0.082 (0.480)	5.03e ⁻⁴	
Left middle temporal cortex	0.696 \pm 0.123	0.708 \pm 0.132	-0.021 [-0.043; 0.001]	-1.920	0.056 (0.081)	0.012	-0.021 [-0.044; 0.002]	-1.787	0.075 (0.104)	0.012	-0.001 [-0.006; 0.004]	-0.461	0.645 (0.752)	-2.86e ⁻⁵	
Right middle temporal cortex	0.715 \pm 0.137	0.740 \pm 0.140	-0.023 [-0.047; 0.001]	-1.884	0.061 (0.081)	0.012	-0.023 [-0.048; 0.002]	-1.766	0.078 (0.104)	0.010	0.001 [-0.004; 0.006]	0.432	0.666 (0.752)	-1.71e ⁻⁶	

Note: After acquisition and processing of data through the longitudinal pipeline, a quality control check was performed; only 302 subjects were considered having acceptable to optimal data A β -PET.

Abbreviations: A β = amyloid beta; PET = Positron Emission Tomography; M0 = baseline; M24 = two-year follow-up; SD = standard deviation; SUVR = standardized uptake value ratio.

*Linear model was used to test the effect of baseline plasma YKL-40 concentration

**Linear mixed model was used to test the main effect and time interaction of baseline plasma YKL-40 concentration

Table 4. Associations between 1-year changes of plasma YKL-40 concentrations and cognitive performances at M24 and over 2-years changes.

	M24*				2-years changes*			
	Coefficient [95% CI]	Statistic**	P-value	Cohen's f ²	Coefficient [95% CI]	Statistic**	P-value	Cohen's f ²
MMSE	0.217 [-0.079 ; 0.515]	1.433	0.152	-0.007	0.287 [-0.160 ; 0.734]	1.267	0.207	0.007
Verbal Fluency	0.562 [-1.858 ; 2.981]	0.458	0.648	-0.002	-0.502 [-2.734 ; 1.730]	-0.443	0.658	9.59e ⁻⁴
TMTB-TMTA	-3.672 [-13.988 ; 6.643]	-0.702	0.484	-0.019	6.955 [-2.858 ; 16.769]	1.397	0.164	0.009
FCSRT	0.308 [0.044 ; 0.574]	2.280	0.023	0.005	-0.325 [-1.035 ; 0.386]	-0.902	0.368	0.004

Abbreviations: FCSRT = Free and Cued Selective Reminding Test; M24 = two-year follow-up; MMSE = Mini-mental state; TMT = Trail Making Test.

*Linear model was used to test the effect of 1-year changes of plasma YKL-40 concentration.

** t-value or, for MMSE and FCSRT, z-value